Geospatial risk assessment of *Dirofilaria immitis* in mountainous areas of Gilan province using Geographic Information System (GIS)

Fatemeh Manshori Ghaishghorshagh[1], Fateme Jalousian[1]*, Seyed Hossein Hosseini[1], Parviz Shayan[1], Saied Bokaie[2]

[1]Department of Parasitology, Faculty of Veterinary Medicine, University of Tehran, Tehran, Iran
[2] Department of Food Hygiene and Quality Control, Faculty of Veterinary Medicine, University of Tehran, Tehran, Iran

Abstract
The study aimed to investigate the correlation between elevation and various environmental factors influencing *Dirofilaria immitis* (*D. immitis*) infection rate in stray dogs within the mountainous areas of Gilan province, Iran. This study was conducted from 2022 to 2023 and analyzed 392 stray dogs across 12 cities, categorizing them based on elevation and examining variables such as temperature, precipitation, and humidity. The diagnosis of *D. immitis* was performed using PCR methods, and data were processed with ArcGIS 10.8 software. The results revealed an overall infection rate of 44.28% ± 2.73, with Fuman-Masuleh reporting the highest at 60%, and Lahijan recorded the lowest at 25.5%. Linear regression analysis indicated a moderately positive correlation between *D. immitis* cases and elevation (β coefficient of 0.543). Maximum temperature showed a strong positive correlation with *D. immitis* cases (β coefficient of 0.907). Spatial analysis using Moran's I Index indicated no significant spatial autocorrelation between positive cases and elevation, suggesting that temperature and other environmental factors are critical in the distribution of *D. immitis*. The Inverse Distance Weighting (IDW) interpolation highlighted areas at higher risk for *D. immitis* infection, particularly along Gilan province's eastern and western borders. In conclusion, this study highlights the significant infection rate of *D. immitis* infection in stray dogs, even in the mountainous regions of Gilan province. It is crucial to recognize Gilan as a high-risk area for this infection. Therefore, implementing effective control and prevention programs is essential.

Introduction

D.immitis, also known as heartworm, is a parasitic nematode that primarily infects dogs but can also infect felids, wild canids, and humans (although, very rarely) (1). Domestic dogs and wild canids are the primary reservoirs for *D.immitis*. Gilan province is an endemic area for this parasite, with a frequency exceeding 70% in various regions (2). At

least 22 mosquito species are known to have the potential to transmit *D.immitis* in some endemic areas, according to Vezzani and Carbajo (2006). Similarly, in Gilan province, which is an endemic area in Iran, 18 mosquito species that serve as intermediate hosts for *D. immitis* have been identified, as reported by Azari Hamidian et al. (2018), the most common species were *Culex* (Cx.) *theileri* (23.59%), *Cx. tritaeniorhynchus* (20.75%), *Cx. pipiens* (19.37%), *Aedes* (Ae.) *vexans* (18.18%), *Anopheles* (An.) *pseudopictus* (10.92%), and *An. maculipennis* (5.48%) (3). Climate change has been identified as a contributing factor to the observed increases in heartworm prevalence in dogs, as it allows for faster development of the parasite to the infective larval stage in mosquitoes, according to Ledesma and Harrington (4). Additionally, a temperature increase can enable the parasite to establish itself in new areas, as mosquitoes can expand their geographic range, as reported by Sassnau et al. (5). Furthermore, climate change can lengthen the annual transmission season by extending the periods when temperatures are sufficient for parasite development (6). Geographic factors such as elevation and mountain climate may have impacted the heartworm infection prevalence (7, 8). In general, heartworms are less common at higher elevations, as the cooler temperatures are less favorable for the survival and reproduction of the parasite (9). However, climate change is causing temperatures to rise even at higher elevations, which may lead to an increased risk of heartworm transmission in these areas (9). Overall, the influence of climate and geography on the prevalence of heartworm disease is complex and multifaceted. While higher temperatures are generally associated with a higher risk of heartworm, other environmental and geographic factors can also play a role. As climate change continues to alter the environment, it is important to monitor the prevalence of heartworm and other diseases in dogs and other animals and to take appropriate measures to prevent and treat infections (10). Further research is required to develop a more comprehensive understanding of the relationship between precipitation, mosquito populations, climatic factors, and heartworm infection in dogs. The spatial distribution of heartworm infection among dogs in the mountain climate of Gilan province has not yet been assessed. Therefore, this research aimed to evaluate the relationship between altitude, temperature, precipitation, and humidity percent, and the prevalence of *D. immitis* infection in dogs using linear regression statistics and Geographic Information System (GIS) modeling.

Materials and Methods
Study area
A total of 392 blood samples were randomly collected from stray dogs across 12 cities in the mountainous regions of Gilan province from 2022 to 2023 (Table 1). The latitude, longitude, and elevation of the sample collection sites were recorded in Excel spreadsheets. Environmental data, including maximum and minimum annual temperatures, precipitation, and humidity, were obtained from the Iranian Meteorological System (https://www.irimo.ir/eng/index.php). In the mountainous climate of Gilan Province, 12 cities were examined: Astara, Roudbar, Siahkal, Amlash, Somehsara, Rezvanshahr, Talesh, Rasht, Masal, Shaft, and Lahijan.

DNA extraction and polymerase chain reaction (PCR)
The diagnosis of *D. immitis* in these dogs was conducted using the polymerase chain reaction (PCR) method. DNA extraction was performed using the MBST blood DNA Extraction Kit (MBST, Iran), following the manufacturer's instructions. The PCR was carried out with primers F5'-GCTTAATTGATGATGATTGC-3' and R5'-CAAGTGATCCACCGCTAAGAGT-3' designed to amplify a 155 bp partial sequence of the ITS1 locus from *D. immitis* genomic DNA. The PCR master mix was prepared in a total volume of 20 microliters using the master mix (Amplicon, Denmark), along with 1-2 microliters of DNA (adjusted based on DNA quality), and 20 picomoles

of each primer. Amplification was performed using a thermal cycler (Bio-Rad, America) following the time program outlined below: an initial denaturation step at 94°C for 5 minutes, followed by 38 cycles of denaturation at 94°C for 45 seconds, annealing at 51°C for 45 seconds, and extension at 72°C for 45 seconds. An additional elongation step was conducted at 72°C for 5 minutes. The PCR product was evaluated using a 1.5% agarose gel stained with ethidium bromide. Imaging was performed with the Gel Doc XR system (United States), under ultraviolet light.

Statistical Analysis

Data analysis included one-way analysis of variance, and Pearson correlation and linear regression were performed using SPSS version 20 (Tables 1 and 2). The spatial distribution of heartworm infection was mapped according to the administrative divisions by city within the mountainous climate of Gilan province, utilizing ArcGIS software (version 10.8). Spatial analysis was performed on the collected data to identify and visualize areas with high and low infection rates of *D. immitis* in dogs, including spatial autocorrelation, the Moran's I index, and inverse distance weighting (IDW) interpolation conducted using ArcGIS 10.8.

Results

The detection of *D. immitis* DNA in blood samples from 392 dogs across 12 cities in Gilan province revealed a 44.28% ± 2.73 (174/392) infection rate. A positive linear relationship was observed between *D. immitis* cases and elevation, while a strong correlation existed between maximum temperature and positive cases. The spatial distribution map indicated varying infection rates across cities, with Fuman-Masuleh showing the highest prevalence (60%). The input data includes point locations where *D. immitis* has been identified, primarily through PCR diagnostic testing. The IDW interpolation method estimates the continuous distribution of the parasite across the mapped area

by considering the proximity and density of the positive sample points.

Moran's I Index values between -0.030892 and 0.129107 suggest that there is little to no significant clustering of similar values. A Moran's I index close to zero typically indicates a random spatial distribution of the variable being analyzed. The Z-scores ranged from 0.78 to 1.39 and the *P-values* ranged from 0.16 to 0.44, all of which exceed the conventional significance threshold of 0.05 indicating that the results are not statistically significant, meaning there is no spatial autocorrelation between positive cases and elevation. It can be concluded that there is no significant spatial autocorrelation between positive cases and elevation. The data suggests that the distribution of positive cases does not exhibit a systematic pattern related to elevation in the studied mountainous climate of Gilan province.

Discussion

In this study, we evaluated *D. immitis* in stray dogs residing in the mountainous regions of Gilan province, the minimum elevation recorded was 7 meters in Talesh city, while the maximum reached 1,447 meters in Roudbar city, resulting in a mean elevation of 236 ± 14.05 meters. The mean infection rate in this mountainous climate was 44.28% ± 2.73. The maximum temperature was 19.82 ± 1.5°C, and the minimum temperature was 11.86 ± 1.5°C, resulting in a temperature difference of 7.96°C. Additionally, the mean precipitation was 2,769 ± 405.46 mm, and the relative humidity was measured at 75.93% ± 2.9. All of these factors create suitable and ideal conditions for vector mosquitoes and the parasites responsible for the infection rate of approximately 44%. The hot spot map of *D. immitis*-positive cases in Gilan province, Iran, provides valuable insights into the geographical distribution of this parasitic infection among dogs in a mountainous climate. The map visually represents the varying infection rates across different cities, with Fuman-Masuleh exhibiting the highest infection rate of 54-60% and

Lahijan having the lowest at 1-25% (Table1 and Figure 1).

Table1. Data for cities in the mountainous regions of Gilan: mean elevation, temperature, precipitation, and relative humidity by percentage of positive PCR cases

Name of Cities (No. of tested samples)	Positive cases by PCR method (%)	Mean Elevation (Meter)	Mean Temperature		Mean Precipitation (mm³)	Average Relative Humidity (%)
			Max. Temp.(ºC)	Min. Temp.(ºC)		
Fuman-Masoule (n=32)	60	1081	14.78±7.8 %95CI (13.2-16.4)	6.78±5.2 %95CI (5.7-7.8)	2849±4800 %95CI (1868-3829)	81.9±21.6 %95CI (77.5-86.3)
Astara (n=34)	53.3	22	17.41±5.9 %95CI (16.2-18.6)	10.35±4.45 %95CI (9.4-11.3)	3665±7200 %95CI (2132- 5197)	82.6±9.4 %95CI (80.7-84.5)
Roudbar (n=32)	52.6	1447	16.28±7.93 %95CI (14.6-17.9)	5.01±5.14 %95CI (3.9-6.1)	6772±1900 %95CI (6383-5197)	63.8±12.8 %95CI (61.2-66.4)
Siahkal (n=33)	48.2	42	29.2±1.4 %95CI (28.4-29.9)	19.2±1 %95CI (18.6-19.8)	1805±3300 %95CI (1130- 2479)	80± 12.2 %95CI (77.5-82.5)
Amlash (n=32)	46.1	13	29.2±2.2 %95CI (27.9-30.4)	22.6±1.4 %95CI (21.8-23.4)	1829±2600 %95CI (1294-2357)	76±12.2 %95CI (73.5-78.5)
Somehsara (n=32)	45.4	19	11.94±4.89 %95CI (9.6-14.3)	5.73±2.86 %95CI (4.4-7.1)	1941±4800 %95CI (960-2921)	83±11.5 %95CI (80.6-85.3)
Reazvanshar (n=33)	45	15	23.4±4.1 %95CI (22.5-24.2)	15.4±4.1 %95CI (14.6-16.2)	2242±4800 %95CI (1261-3222)	85±12.3 %95CI (82.5-87.5)
Talesh (n=32)	44.1	7	18.35±5.9 %95CI (17.1-19.5)	10.9±4.46 %95CI (9.9-11.8)	3361±6600 %95CI (2012-4709)	77±12.3 %95CI (74.5-79.5)
Rasht (n=35)	43.1	24.8	19.77±7.04 %95CI (18.3-21.2)	10.9±4.4 %95CI (9.4-11.2)	2294±4800 %95CI (1313-3274)	82.9±11.6 %95CI (80.5-85.3)
Masal (n=32)	34.7	80	21.9±7.91 %95CI (20.3-23.5)	12.2±4.9 %95CI (11.19- 13.2)	1780±4317 %95CI (897- 2662)	75±12.2 %95CI (72.5-77.5)
Shaft (n=33)	33.3	47	24.5±1.3 %95CI (23.8-25.2)	13.7±1.2 %95CI (13-14.4)	2643±3350 %95CI (1958-3327)	51±12.8 %95CI (48.4-53.6)
Lahijan (n=32)	25.5	34.2	20.46±7.09 %95CI (19-21.9)	9.52±4.23 %95CI (8.6-10.4)	2047±4700 %95CI (1086- 3007)	79±12.8 %95CI (76.4-81.6)

The linear regression analysis revealed a positive linear relationship and moderate correlation between the positive cases of *D. immitis* and elevation (β coefficients = 0.543, *p* = 0.07, r = 0.5). The maximum temperature and the number of positive *D. immitis* cases were found to have a strong positive linear relationship (β coefficients = 0.907, r = 0.9, *p* = 0.01). The maximum precipitation and average relative humidity showed a positive linear relationship and weak correlation with positive cases of *D. immitis* (β coefficient = 0.314, r = 0.335, *p* = 0.32).

Table2. Mean infected cases of cities by elevation group, with ANOVA results

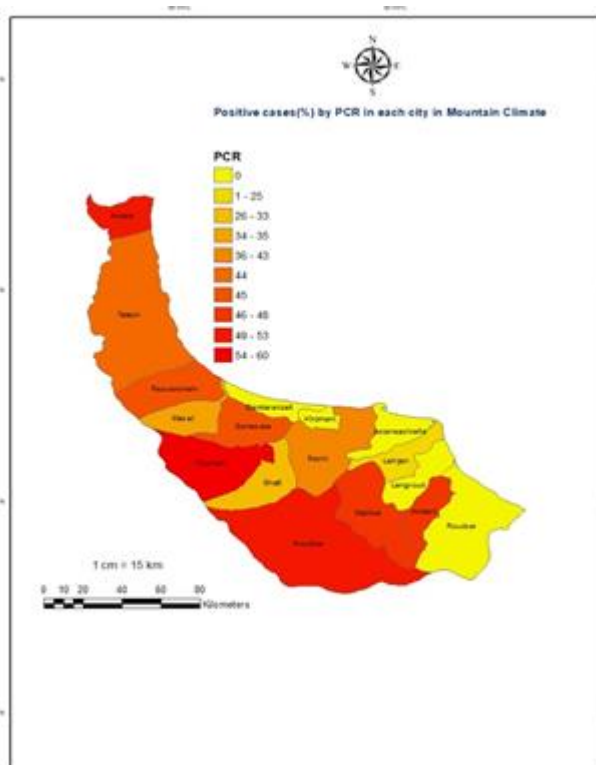| Elevation (m)	Name of Cities	Mean of infected cases (%) ±SD	Post Hoc Tukey HSD	ANOVA
G1: $\leq$ 20 m	Amlash, Somesara, Rezvanshahr, Talesh	45.5 ± 1.03	G1:G2 4.79 Q=1.26; p=0.65	F=2.73 p=0.1
G2: $\leq$ 21-50 m	Astara, Siahkal, Rasht, Shaft, Lahijan	40.7 ± 11.2	G2:G3 12.78 Q=3.36; p=0.08	
G3: $\geq$ 51 m	Fouman, Roudbar, Masal	53.5 ± 10.9	G3:G1 7.99 Q=2.1; p=0.33	

Fig. 1. Hot Spots Map of *Dirofilaria immitis*(*D.immitis*) Positive Cases in Gilan Province, Iran. From dark red to light red, the distribution is as follows: Fuman-Masuleh (54-60%), Astara, Roudbar, Siahkal (49-53%), Amlash (46-48%), Somehsara, Rezvanshahr (45%), Talesh (44%), Rasht (36-43%), Masal (34-35%), Shaft (26-33%), Lahijan (1-25%).
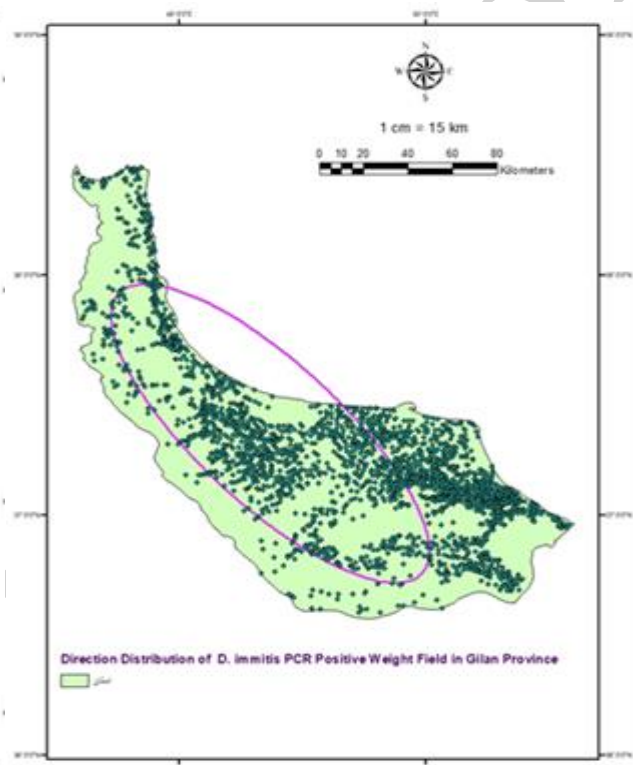
Fig. 2. Direction distribution of *Dirofilaria immitis* Weight Field in Gilan province (ArcGIS 10.8). This map displays the directional distribution of the weight field for *D. immitis* in Gilan province, created using ArcGIS 10.8. The circle indicates the predominant directions north-to- south of *D. immitis* distribution, providing insights into the patterns of infection within the region.
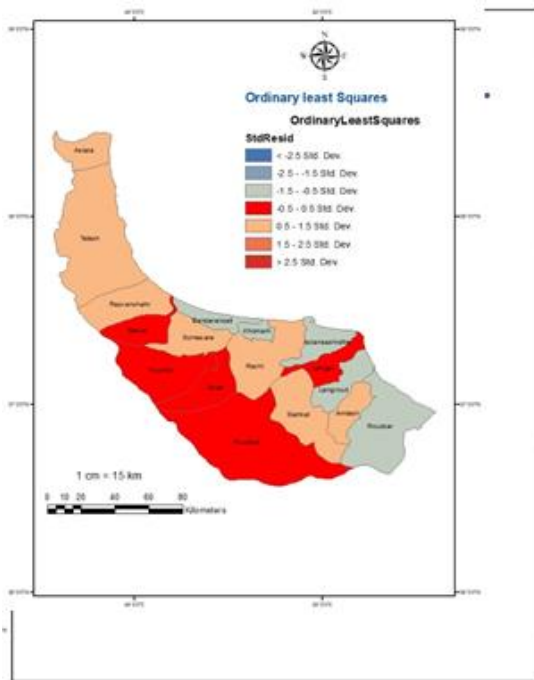
Fig. 3. Standard Residuals from Ordinary Least Squares Analysis (ArcGIS 10.8). The spectrum of red color represents areas where observed values are higher than predicted. Negative Residuals: Shown in the spectrum of blue to gray, indicating areas where observed values are lower than predicted. This visualization helps identify patterns of deviation from the regression model across the study area.
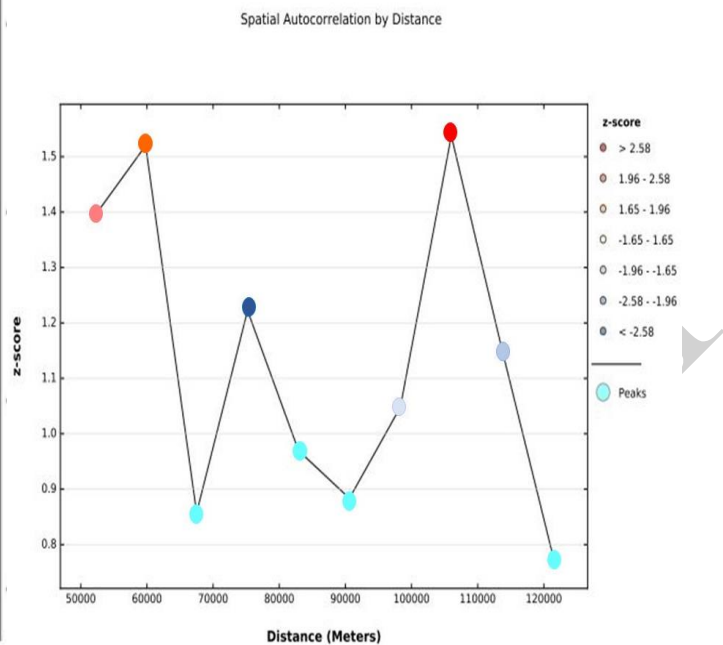
Fig. 4. Spatial Autocorrelation by Distance. This graph illustrates the relationship between distance and spatial autocorrelation, specifically focusing on the Z-scores derived from the analysis. The positive Z-scores observed for all cities with positive cases of *D. immitis* indicate a tendency for clustering of similar values at those distances.

Table3. Table of elevation, Moran's I index, Z-Score, and *P*-value data

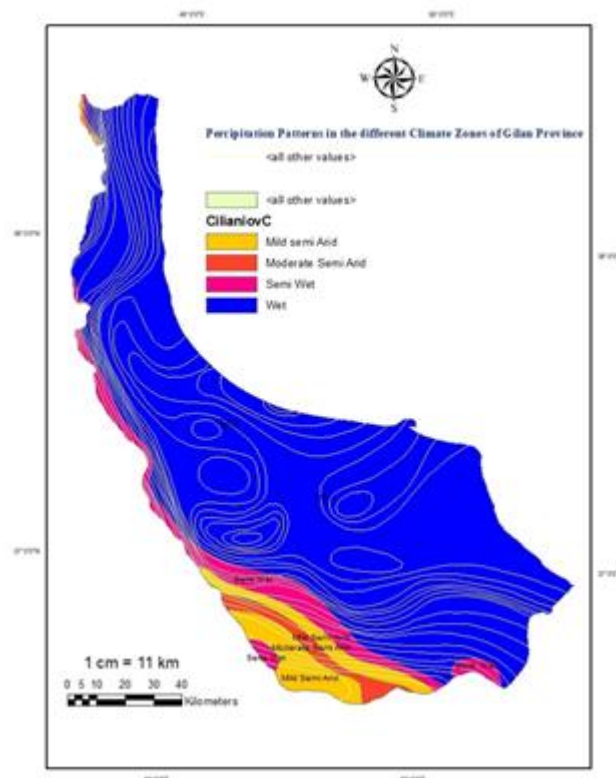| Elevation	Moran's I Index	Z-score	*P-value*
52112	0.129107	1.39	0.16
59812.33	0.124052	1.52	0.13
67512.65	0.031185	0.86	0.39
75212.98	0.052704	1.22	0.22
82913.31	0.025561	0.97	0.33
90613.63	0.011804	0.88	0.38
98313.96	0.006037	1.05	0.29
106014.29	0.025453	1.54	0.12
113714.61	- 0.007464	1.15	0.25
121414.94	- 0.030892	0.78	0.44

Fig. 5. Precipitation patterns in different zones of Gilan province, Iran. This map illustrates the spatial distribution of precipitation patterns across various zones within Gilan province. The map highlights the differences in precipitation regimes between these zones, providing insights into the geographic variability of rainfall in Gilan province.
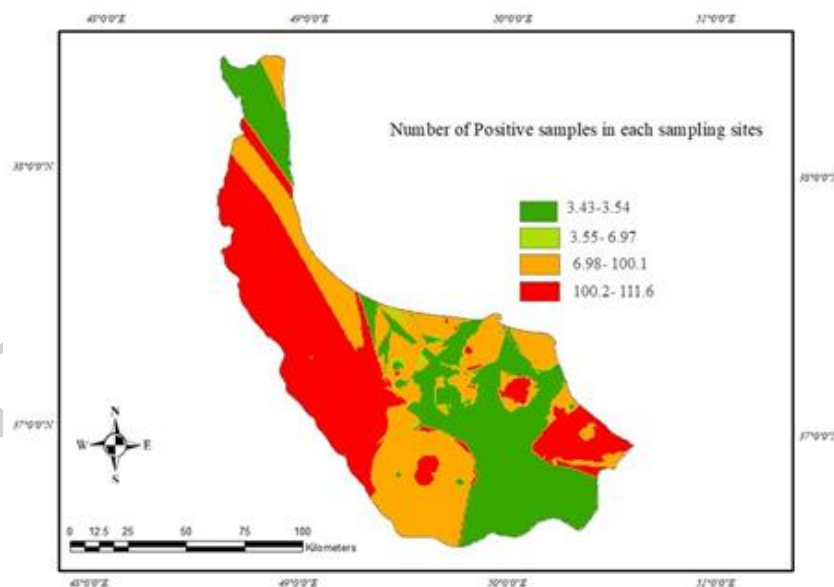

Fig. 6. Map of continuous spatial distribution of *Dirofilaria immitis* in Gilan province (2022-2023). The map shows the spatial distribution of *D. immitis* using IDW interpolation (Arc GIS 10.8). The input data consists of point locations where *D. immitis* has been detected, primarily based on PCR diagnostic testing. The IDW interpolation estimates the continuous distribution of the parasite across the mapped area based on the proximity and density of the positive sample points.

The cities, in mountainous areas, were categorized into three groups based on their elevation:

Group 1 (G1) includes cities with elevations less than or equal to 20 meters, with a mean infection rate of 45.5%; Group 2 (G2) consists of cities with elevations between 21 and 50 meters, showing a mean infection rate of 40.7%; and Group 3 (G3) comprises cities with elevations greater than or equal to 51 meters, where the mean infection rate was approximately 53.5% (Table 2).

ANOVA analysis indicated no significant difference in the infection rates between the groups at a *p*-value of <0.05. Post Hoc Tukey HSD analysis revealed that the maximum differences in infection rates were observed between G2 and G3, followed by differences between G1 and G3, and finally between G1 and G2. These results suggest that factors other than elevation may also influence the infection rate of *D. immitis* in this climate (Table 2). The correlation between climate and the distribution of positive cases aligns with existing literature, highlighting how warmer and more humid conditions facilitate the lifecycle of *D. immitis* and its vectors, primarily mosquitoes (11, 12).

The significant variation in the infection rates among the studied cities suggests that local ecological conditions, including elevation, temperature, and humidity, play a crucial role in influencing the prevalence of this disease. However, the ANOVA analysis revealed no significant differences (*p* >0.05) (Table 2), indicating that the observed variations may not be statistically significant (Tables 1 and 2). The linear regression analysis showed a positive linear relationship and a moderate correlation between the positive cases of *D. immitis* and elevation (β coefficient = 0.543, *p* = 0.07, r = 0.5). This suggests that as elevation increases, the number of positive cases tends to increase as well, although the correlation is not statistically significant at the 0.05 level (Tables 1 and 2).

In contrast, the analysis revealed a strong positive correlation between the maximum temperature and the cases of D. *immitis*. The β coefficient was 0.907, the r-value was 0.9, and the p-value was 0.01, indicating a significant relationship. This significant relationship suggests that higher maximum temperatures are associated with an increased number of positive cases (Tables 1 and 2). Furthermore, the analysis of maximum precipitation and average relative humidity demonstrated a positive linear relationship with the positive cases of *D. immitis*, although the correlation was weak. The β coefficient was 0.314, with an r-value of 0.335 and a p-value of 0.32, indicating that these factors have a less significant effect on the infection rates (Tables 1 and 2).

Understanding the hotspots of infection allows for targeted interventions, such as increased veterinary care in high-prevalence areas, public awareness campaigns about the risks of *D. immitis*, and vector control initiatives (13). In conclusion, the hot spot map and statistical analyses provide valuable insights into the geographical distribution and environmental factors associated with *D. immitis* infection in Gilan province.

The directional distribution observed in Figure 2 may also reflect the movement patterns of both canine hosts and mosquito vectors. As dogs and other canids roam within these areas, they may contribute to the spread of *D. immitis*, particularly when they are not receiving adequate veterinary care or preventive treatments. The north-to-south trend could suggest that certain cities or areas along this axis have higher populations of the infected dogs, which may serve as reservoirs for the parasite (Figure 2)

The standardized residuals are color-coded to indicate both the magnitude and direction of the deviations from the regression model. Positive residuals, represented by shades of red, highlight areas such as Roudbar and Shaft, Lahijan, Fouman, and Masal where the observed values of *D. immitis* cases are higher than predicted by the model. This

suggests that these locations may have unique characteristics or environmental factors contributing to increased infection rates that were not fully captured by the explanatory variables included in the OLS analysis (Figure 3).

Conversely, negative residuals are depicted in shades of gray, indicating areas where the observed values are lower than predicted, possibly due to missing variables or local conditions that mitigate the transmission of *D. immitis*. The visualization of standardized residuals is crucial for assessing the fit of the regression model. A well-fitting model should yield residuals that are randomly distributed around zero, without significant clustering of high or low values (Figure 3). Moreover, the identification of these patterns can guide further research and data collection efforts.

The presence of positive Z-scores suggests that there is some degree of clustering among cities with positive cases of *D. immitis*. This clustering may imply that certain areas are more affected than others, potentially due to localized environmental factors or demographic characteristics that facilitate the transmission of the parasite. However, Moran's I Index values, which ranged from -0.030892 to 0.129107, indicate little to no significant clustering of similar values (Table 3). A Moran's I index close to zero typically points to a random spatial distribution of the variable being analyzed, suggesting that while there may be some clustering, it is not strong enough to indicate a significant spatial pattern (Table 3 and Figure 4).

The Z-scores ranged from 0.78 to 1.39, and the *p*-values ranged from 0.16 to 0.44, all exceeding the conventional significance threshold of 0.05. This indicates that the results are not statistically significant, reinforcing the conclusion that there is no meaningful spatial autocorrelation between positive cases of *D. immitis* and elevation. The lack of significant spatial autocorrelation suggests that the distribution of positive cases does not exhibit a systematic pattern related to elevation in the mountainous climate of Gilan province (Table 3) (Figure 4).

While, the analysis indicates some clustering of *D. immitis*-positive cases, the lack of significant spatial autocorrelation with elevation suggests that the distribution of infections is influenced by a complex interplay of factors. Further investigation into these variables will be essential to develop effective control strategies and improve our understanding of the epidemiology of *D. immitis* in mountainous regions.

The precipitation map of Gilan province illustrates the mean precipitation in the mountainous climate to be approximately $2,769 \pm 405.4$ mm^3, with a relative humidity of $75.93\% \pm 2.9$. This high rainfall and humidity create an ideal environment for mosquito vectors and the transmission of *D. immitis*. (Figure 5). West and southwest of Roudbar experiences, semi-wet, moderate semi-arid, and mild semi-arid while simultaneously reporting a high infection rate of *D. immitis* (52.6%) suggests that in Roudbar, the relatively 6772 ± 1900 mm^3 rainfall and $63.83 \pm 12.8\%$ relative humidity and the difference between maximum and minimum temperature about 11.27ºC is a critical factor to consider. The low-temperature variation in Roudbar may create a conducive environment for mosquito populations, this aligns with findings from other studies that highlight temperature as a significant factor influencing the incidence of vector-borne diseases, including malaria, where higher temperatures have been linked to increased transmission rates. Furthermore, the ecological characteristics of Roudbar, such as the presence of suitable breeding sites for mosquitoes relative to annually rainfall, may also play a crucial role in the observed infection rates (Figure 5).

The strong correlation (β coefficient of 0.907, r-value of 0.9, and p-value of 0.01) suggests that higher maximum temperatures create favorable conditions for the lifecycle of both *D. immitis* and its mosquito vectors (13). Warmer temperatures can lead to increased mosquito activity, higher reproductive rates, and extended transmission seasons, thereby elevating the risk of infection in canine populations (13). Understanding the impact

of temperature on infection rates can inform public health strategies. Regions experiencing higher temperatures may require intensified surveillance and preventive measures, such as increased veterinary care, public awareness campaigns, and vector control initiatives (14). By focusing resources on high-risk areas, stakeholders can more effectively mitigate the spread of *D. immitis* (14). As global temperatures rise due to climate change, the potential for increased *D. immitis* transmission may expand beyond current endemic areas (15). This underscores the need for ongoing research into how changing climatic conditions may alter the epidemiology of vector-borne diseases, prompting proactive measures to address emerging risks (15). The findings highlight the importance of considering temperature as a critical environmental factor influencing *D. immitis* prevalence (16). This knowledge can guide further research into the interactions between temperature, humidity, and other ecological variables that affect the distribution and transmission dynamics of the parasite (17). The relationship between temperature and infection rates emphasizes the need for long-term monitoring of both climatic conditions and *D. immitis* prevalence (17). By integrating climate data with epidemiological studies, researchers can develop predictive models to anticipate changes in infection patterns and inform public health planning (17). The map depicting the continuous spatial distribution of *D. immitis* in Gilan province, using IDW interpolation, provides valuable insights into the potential risk areas for this parasitic infection. By incorporating point locations where *D. immitis* has been detected, primarily through PCR diagnostic testing, the map estimates the continuous distribution of the parasite across the region based on the proximity and density of the positive sample points (Figure 6). The IDW interpolation technique employed in this analysis is a powerful tool for visualizing the potential spread of *D. immitis* in Gilan province (18).

By considering the spatial relationships between positive sample points, the map identifies areas at high risk for infection, particularly along the eastern and western borders of the province (Figure 6). This information is crucial for public health authorities and veterinary professionals to prioritize surveillance, prevention, and control measures in these high-risk regions (19).

The map aligns with previous studies that have identified Gilan province as an endemic area for dirofilariasis, with a high prevalence of *D. immitis* infections in canine populations (20). The humid subtropical climate of the region, characterized by high rainfall and moderate temperatures, provides an ideal environment for the mosquito vectors that transmit the parasite (20). Additionally, vector control measures, such as mosquito abatement programs, can be prioritized in the identified high-risk regions to reduce the potential for transmission (21). Furthermore, the continuous spatial distribution map serves as a valuable tool for monitoring the spread of *D. immitis* over time, by regularly updating the map with new data from PCR testing and surveillance efforts, researchers and public health officials can track changes in the distribution patterns and identify emerging hotspots (22).

The prevalence of infectious diseases in mountainous climates is influenced by a complex interplay of environmental factors, including temperature, humidity, and the presence of suitable vectors or reservoirs. Understanding these dynamics is crucial for intervention strategies aimed at controlling the spread of these diseases in vulnerable populations (23). While malaria is more commonly associated with tropical climates, certain mountainous regions in Africa and Asia experience malaria transmission due to the presence of specific mosquito species that thrive in cooler, higher-altitude environments. Changes in climate, such as increased rainfall and temperature, can also expand the range of malaria-carrying mosquitoes into previously unaffected mountainous areas (24). *Hantavirus* is primarily transmitted through contact with rodent droppings, urine, or saliva. In mountainous regions, where rodent populations

may thrive in cooler climates, the risk of the disease can increase. The combination of environmental factors such as altitude, temperature, and humidity can influence rodent behavior and habitat, subsequently affecting the transmission risk to humans (25). Lyme disease, caused by the bacterium *Borrelia burgdorferi*, is transmitted through tick bites. In mountainous areas, the presence of dense forests and underbrush provides a suitable habitat for ticks and their animal hosts. The higher elevation and cooler temperatures can also influence the seasonal activity of ticks, making certain mountainous regions hotspots for Lyme disease transmission (26). Leptospirosis infection is more prevalent in mountainous regions, particularly in tropical and subtropical areas. The disease is transmitted through water contaminated with the urine of infected animals. In mountainous climates, heavy rainfall and flooding can lead to increased exposure to contaminated water sources, raising the risk of infection (27). The interplay of environmental factors in mountainous regions, including climate conditions, elevation, vector dynamics, local ecology, and human-animal interactions, plays a crucial role in the spread of infectious diseases like filariasis. Understanding these relationships is essential to developing effective public health interventions and controlling the transmission of vector-borne diseases in these unique environments (28).

Conclusion

Overall, the study highlights the importance of geographic variables, particularly altitude and precipitation, in influencing the prevalence and distribution of *D. immitis* infection in mountainous regions. The findings provide valuable insights for public health officials and researchers working towards mitigating the impact of *D. immitis* and other vector-borne diseases in similar environments.

References

1. Vezzani D, Carbajo AE. Spatial and temporal transmission risk of Dirofilaria immitis in Argentina. Int J Parasitol. 2006;36(14):1463-72. http://doi.org/10.1016/j.ijpara.2006.08.012

2. Hosseini SH, Manshori-Ghaishghorshagh F, Ramezani M, Nayebzadeh H, Ahoo MB, Eslamian A, et al. Canine microfilaraemia in some regions of Iran. Parasit Vectors. 2022; 15 (1):90.https://doi.org/10.1186/s13071-022-05209-7

3. Azari-Hamidian S, Norouzi B, Noorallahi A, Hanafi-Bojd AA. Seasonal activity of adult mosquitoes (Diptera: Culicidae) in a focus of dirofilariasis and West Nile Infection in northern Iran. J Arthropod Borne Dis. 2018; 12 (4):398.http://doi.org/10.1111/j.1365-2915.2009.00802.x.

4. Ledesma N, Harrington L. Fine-scale temperature fluctuation and modulation of *Dirofilaria immitis* larval development in Aedes aegypti. Vet Parasitol. 2015; 209 (1-2):93-100. http://doi.org/10.1016/j.vetpar.2015.02.003

5. Sassnau R, Czajka C, Kronefeld M, Werner D, Genchi C, Tannich E, et al. Dirofilaria repens and *Dirofilaria immitis* DNA findings in mosquitoes in Germany: temperature data allow autochthonous extrinsic development. Parasitol Res. 2014; 113:3057-61. https://doi.org/10.1007/s00436-014-3970-1

6. Alho AM, Meireles J, Schnyder M, Cardoso L, Belo S, Deplazes P, et al. *Dirofilaria immitis* and Angiostrongylus vasorum: The current situation of two major canine heartworms in

Portugal. Vet Parasitol. 2018; 252:120-6. http://doi.org/10.1016/j.vetpar.2018.01.008

7. Constantinoiu C, Croton C, Paterson MB, Knott L, Henning J, Mallyon J, et al. Prevalence of canine heartworm infection in Queensland, Australia: comparison of diagnostic methods and investigation of factors associated with reduction in antigen detection. Parasit Vectors. 2023; 16 (1):63. http://doi.org/10.1186/s13071-022-05633-9

8. Herrin BH, Peregrine AS, Goring J, Beall MJ, Little SE. Canine infection with Borrelia burgdorferi, *Dirofilaria immitis*, Anaplasma spp. and Ehrlichia spp. in Canada, 2013–2014. Parasit Vectors. 2017; 10: 1-9. https://doi.org/10.1186/s13071-017-2184-7

9. Bowman DD, Liu Y, McMahan CS, Nordone SK, Yabsley MJ, Lund RB. Forecasting United States heartworm *Dirofilaria immitis* prevalence in dogs. Parasit Vectors. 2016 Dec; 9:1-2.https://doi.org/10.1186/s13071-016-1804-y

10. Negron V, Saleh MN, Sobotyk C, Luksovsky JL, Harvey TV, Verocai GG. Probe-based qPCR as an alternative to modified Knott's test when screening dogs for heartworm (*Dirofilaria immitis*) infection in combination with antigen detection tests. Parasit Vectors. 2022;15(1):306.
https://doi.org/10.1186/s13071-022-05372-x

11. Jitsamai W, Piromkij P, Kamkong P, Chungpivat S, Taweethavonsawat P. Seasonal distribution and environmental parameters associated with Brugia pahangi and *Dirofilaria immitis* in naturally infected dogs in Bangkok and vicinity, Thailand. Sci Rep. 2021; 11(1):4594. https://doi.org/10.1038/s41598-021-84215-8

12. Riahi SM, Yusuf MA, Azari-Hamidian S, Solgi R. Prevalence of in mosquitoes (Diptera)– systematic review and meta-analysis. J Nematol.2021;53(1):1-3. https://doi.org/10.21307/jofnem-2021-012

13. Montoya-Alonso JA, García-Rodríguez SN, Matos JI, Costa-Rodríguez N, Falcón-Cordón Y, Carretón E, et al. Change in the Distribution Pattern of *Dirofilaria immitis* in Gran Canaria (Hyperendemic Island) between 1994 and 2020. Animals. 2024; 14(14):2037. https://doi.org/10.3390/ani14142037

14. Hoseini M, Jalousian F, Hoseini SH, Sadeghian AG. A cross sectional study on *Dirofilaria immitis* and Acanthocheilonema reconditum in sheepdogs in a western region in Iran. Vet Res Forum.2020;11(2):185-190. . https://doi.org/10.30466/vrf.2018.78930.2046

15. Anvari D, Saadati D, Siyadatpanah A, Gholami S. Prevalence of dirofilariasis in shepherd and stray dogs in Iranshahr, southeast of Iran. J Parasit Dis. 2019; 43: 319-23. https://doi.org/10.1007/s12639-019-01096-5

16. Sharifdini M, Karimi M, Ashrafi K, Soleimani M, Mirjalali H. Prevalence and molecular characterization of *Dirofilaria immitis* in road killed canids of northern Iran. BMC Vet Res. 2022;18(1):161
https://doi.org/10.1186/s12917-022-03270-z

17. Ashwini M, Talluri Rameshwari KR, Sumana MN, Sumana K. GIS-Based analysis of the spatial distribution of dengue disease in Mysuru district and India, 2013-2018. Int J Mosq Res. 2020;7(6):13-26.
https://doi.org/10.22271/23487941.2020.v7.i6a.484

18. Javaid M, Sarfraz MS, Aftab MU, Zaman QU, Rauf HT, Alnowibet KA. WebGIS-Based Real-Time Surveillance and Response System for Vector-Borne Infectious Diseases. Int J Environ Res Public Health. 2023; 20(4):3740. https://doi.org/10.3390/ijerph20043740

19. Pergantas P, Papanikolaou NE, Malesios C, Tsatsaris A, Kondakis M, Perganta I, et al. Towards a semi-automatic early warning system for vector-borne diseases. Int J Environ Res Public Health. 2021; 18 (4):1823. . https://doi.org/10.3390/ijerph18041823

20. Malmasi A, Hosseini SH, Aramoon M, Bahonar A, Seifi HA. Survey of canine *Dirofilaria immitis* infection in Caspian provinces of Iran. Iran J Vet Res. 2011; 12 (4):340-4.
http://doi.org/10.22099/IJVR.2011.87

21. Agayev I, Vahabov E, Jalilov V, Moradi-Asl E, Saghafipour A. Epidemiological situation and spatial distribution of visceral leishmaniasis in the Republic of Azerbaijan. J Parasit Dis. 2020; 44:639-45.https://doi.org/10.1007/s12639-020-01242-4

22. Oh IY, Kim KT, Sung HJ. Molecular detection of *Dirofilaria immitis* specific gene from infected dog blood sample using polymerase

chain reaction. Iran J Parasitol. 2017; 12(3):433.

23. Basnyat B, Cumbo TA, Edelman R. Infections at high altitude. Clin Infect Dis. 2001;33(11):1887-91. https://doi.org/10.1086/324163

24. Mafwele BJ, Lee JW. Relationships between transmission of malaria in Africa and climate factors. Sci Rep. 2022; 12(1):14392. https://doi.org/10.1038/s41598-022-18782-9

25. Douglas KO, Payne K, Sabino-Santos Jr G, Agard J. Influence of climatic factors on human Hantavirus infections in Latin America and the Caribbean: a systematic review. Pathogens. 2021;11(1):15. https://doi.org/10.3390/pathogens11010015

26. Lantos PM, Tsao J, Janko M, Arab A, Von Fricken ME, Auwaerter PG, et al. Environmental correlates of Lyme disease emergence in Southwest Virginia, 2005–2014. J Med Entomol. 2021; 58(4):1680-5. https://doi.org/10.1093/jme/tjab038

27. Bradley EA, Lockaby G. Leptospirosis and the environment: A review and future directions. Pathogens. 2023; 12 (9):1167. https://doi.org/10.3390/pathogens12091167

28. Kaikuntod M, Arjkumpa O, Kladkempetch D, Fukumoto S, Thongkorn K, Boonyapakorn C, et al. Geographic spatial distribution patterns of *Dirofilaria immitis* and Brugia pahangi infection in community dogs in Chiang Mai, Thailand. Animals. 2020; 11(1):33. https://doi.org/10.3390/ani11010033